

Local Incremental Planning for Nonholonomic Mobile Robots

Alessandro De Luca

Dipartimento di Scienze dell'Informazione
Università di Milano
Via Comelico 39, 20135 Milano, Italy

Giuseppe Oriolo

Dipartimento di Informatica e Sistemistica
Università di Roma "La Sapienza"
Via Eudossiana 18, 00184 Roma, Italy

Abstract

We present a simple approach for planning the motion of nonholonomic robots among obstacles. Existing methods lead to open-loop solutions which are either obtained in two stages, approximating a previously built holonomic path, or computationally intensive, being based on configuration space discretization. Our non-holonomic planner employs a direct projection strategy to modify on-line the output of a holonomic incremental planner, and generates velocity control inputs that realize the desired motion in a least-squares sense. As a result, a feedback scheme is obtained which can use only local sensor information. The proposed approach is applied to unicycle kinematics, with artificial potential fields or vortex fields as local holonomic planners.

1. Introduction

Robots whose motion is subject to non-integrable constraints involving time derivatives of the configuration variables belong to the class of *nonholonomic* mechanical systems [1]. Typical examples are wheeled mobile robots moving on the plane under perfect rolling constraints. The effect of these constraints is to limit the local mobility of the robotic system, though not restricting in the large the accessibility of the whole configuration space.

For nonholonomic robots, the design of feasible trajectories joining arbitrary initial and final configurations is not straightforward, and can be tackled as an intrinsic nonlinear control problem [2]. In this respect, *open-loop* schemes and *feedback* control are possible solutions. Based on a differential geometric analysis, open-loop commands that exactly drive to the goal have been derived in [3-5] for the class of mobile robots that can be put in the so-called chained form. Feedback schemes are indeed more robust but subject to a basic limitation: nonholonomic systems cannot be stabilized to a given configuration by means of a continuously differentiable feedback law, as follows from a general result due to Brockett [6]. This motivated

the more complex design of *discontinuous* [7], *smooth time-varying* [8], or hybrid [9] feedback control laws. A common characteristic of these open- or closed-loop methods is that a sequence of maneuvers is required in order to complete a point-to-point motion, like in parking a car or docking a truck with trailers. The *presence of obstacles* in the operational space is not taken into account at this stage.

On the other hand, for conventional (holonomic) robots the literature on motion planning with obstacle avoidance is quite rich [10]. Two major approaches can be identified, namely *algorithmic* and *incremental* planning. Methods of the first class search for a solution path in the free configuration space, directly facing the combinatorial complexity of the problem. Techniques from real algebraic geometry are used to guarantee completeness, that is finding a solution whenever one exists. The resulting algorithms are powerful but very difficult to implement for high-dimensional configuration spaces. Moreover, shape and location of all obstacles must be known a priori.

Incremental methods are more heuristic in nature but operate in feedback mode, thus being more suitable for sensor-based navigation through partially unknown environments. With the standard *artificial potential field* method, the robot moves under the local effects of repulsive fields associated to obstacles and the attractive field pulling toward the goal [11]. These fields may be defined in the configuration space or, more conveniently, in the cartesian space. One typical limitation is the arising of spurious *local minima* in the total potential field, where no descent direction exists for the motion.

Several modifications have been introduced to overcome this problem, ranging from use of repulsive fields with elliptic isocontours [12], definition of special global fields [13], or generation of a numerical potential field [14]. Another method avoiding the generation of 'motion stops', but which can be defined using only *local* information, is the *vortex field* method [15]. Repulsive actions are there replaced by velocity flows tangent to the isocontours so that the robot is forced

to turn around the obstacles.

Few methods exist that attempt to solve the planning problem taking explicitly into account the nonholonomic constraints and the presence of obstacles [16–18]. All of them are essentially open-loop schemes. In [16,17] a two-stage approach is followed for a car-like robot in the plane: first, generate a complete path avoiding obstacles with any holonomic planner; then, decompose and approximate this path with feasible segments complying with the nonholonomic constraints. A discretization of the configuration space is essential in [18], where graph search based on Dijkstra algorithm is performed.

In this paper we propose a more direct navigation technique for nonholonomic vehicles. The idea is to employ a feasible projection strategy to modify on-line the output of a holonomic incremental planner. The resulting feedback scheme uses only local information, limited e.g. to the range of distance sensors. The crucial feature of this strategy is that it should not create additional blocking points in the configuration space of the nonholonomic vehicle. We highlight the general approach and then apply it to the kinematics of a unicycle, modeling a real mobile robot situation. Simulation results are reported in which artificial potential fields or vortex fields are used in the conventional holonomic planner.

2. Incremental motion planning for nonholonomic robots

We consider the planar motion of a wheeled mobile robot. Denoting by $X \in \mathbb{R}^n$ the vector of generalized coordinates, assume that the system motion is subject to a set of $p < n$ nonholonomic constraints in the form

$$A(X)\dot{X} = 0, \quad (1)$$

that arise in connection with the ‘rolling without slipping’ condition on the wheels. Note that the presence of rolling wheels does not necessarily imply that motion on the plane is subject to nonholonomic constraints. Wheels with side rollers or other complex mechanisms may be used to guarantee omnidirectionality.

Since constraint (1), involving the time derivatives of the generalized coordinates, is not integrable, the dimension of the configuration space cannot be reduced. However, all feasible velocities \dot{X} should satisfy the following equation

$$\dot{X} = G(X)u, \quad u \in \mathbb{R}^{n-p}, \quad (2)$$

where the $n - p$ independent columns of $G(X)$ are a basis for the null space of $A(X)$. Equation (2) is the

kinematic model of the mobile robot. Depending on the choice of the null space basis, the components u_i will have a different meaning. Indeed, there is one choice which leads to a convenient physical interpretation of u in terms of the available commands.

We assume in the following that control inputs are at the velocity level. In practice, this is not restrictive for real mobile robot control. Although the modeling can easily be extended to second order and to include the system dynamics [19], eq. (2) already displays the main difficulty due to nonholonomy. In fact, system (2) is essentially *underactuated*, having strictly less independent inputs u than motion planning variables X .

Given any desired trajectory $X_d(t)$, a straightforward approach is to design the input command u using pseudoinversion

$$u = G^\#(X)\dot{X}_d = [G^T(X)G(X)]^{-1}G^T(X)\dot{X}_d. \quad (3)$$

This solution locally minimizes the error $(\dot{X}_d - \dot{X})$ in a least-squares sense. A weighted pseudoinverse can also be used to balance error components and to handle nonhomogeneous unit dimensions. If the desired velocity \dot{X}_d satisfies the nonholonomic constraint (1) at the current X , eq. (3) will result in zero velocity error. Note that the pseudoinverse is computed using the actual configuration so that the command u is a *feedback* control.

In eq. (3), \dot{X}_d can be chosen as the output of an incremental holonomic planner. If artificial potentials are used to drive the robot, then

$$\dot{X}_d = -\nabla_X U(X) = -\nabla_X (U_a(X) + U_r(X)), \quad (4)$$

with an attractive potential U_a to the goal X_g and a repulsive potential U_r .

However, working with potentials defined in the *whole* configuration space X is computationally inefficient [10]. In view of the planar nature of the motion problem, one can partition X as (X_p, X_θ) , with the positional part $X_p = (x, y) \in \mathbb{R}^2$ and the angular part $X_\theta \in \mathbb{R}^{n-2}$. For example, in a car with N trailers, X_p are the cartesian coordinates of one representative point of the robot (typically, the position of the last trailer [20]), while X_θ contains the orientation and the steer angle of the car as well as the relative orientation of each trailer. Potential fields can then be set up for X_p , i.e., directly in the operational space where obstacles live, by defining several cartesian points $P_i = (x_i, y_i)$ on the (multibody) mobile robot. Each of these *control points* will be subject to a field $U_{a,i} + U_{rep}$, being $U_{a,i}$ the attractive field associated to the goal for P_i . The desired motion becomes

$$\dot{X}_d = -\sum_i J_i^T(X)\nabla_{X_p}(U_{a,i}(P_i) + U_r(P_i)), \quad (5)$$

where $J_i(X)$ is the Jacobian of the kinematic mapping $P_i = f_i(X)$ of the i -th control point.

Substitution of eqs. (4) or (5) in (3) yields a non-holonomic motion planner. Its performance obviously depends on the characteristics of the holonomic planner, but also on the interaction between the latter and the projection scheme. In order to allow for more flexibility in the design, one can then keep the positional part $\dot{X}_{p,d}$ of eq. (5) and specify the desired motion of the angular part in a more general form

$$\dot{X}_{\theta,d} = \Phi(X, \dot{X}_{p,d}), \quad (6)$$

where an explicit dependence of the angular planning on the positional one has been introduced. The design of a suitable Φ is strictly related to the kinematic structure of the vehicle and is critical for the success of the method. In particular, one should guarantee that *no additional blocking points* are generated in the configuration space X of the nonholonomic vehicle, beside those possibly existing for X_p . In Sec. 4 we show how to achieve this for a unicycle.

We note that, as long as the overall feedback law (3) is continuously differentiable, the scheme will not be able to stabilize the mobile robot at a given configuration X_g (or, equivalently, not all control points P_i will reach their final position). In fact, this would violate the theoretical result of Brockett [6], as applied to non-holonomic systems. However, since our objective is the definition of a navigation method among obstacles, we are not interested in the specific configuration reached at the end of the motion, provided that the positional coordinates of the robot reach their destination $X_{p,g}$.

Finally, we point out a possible shortcoming of the method. Since the commands of the holonomic planner are realized only in a least-squares sense, there is no complete guarantee that obstacles will be avoided during motion. Therefore, use of motion safety margins related to the maximum velocity error is advisable.

3. Local holonomic planners

One basic component of the proposed planner is its holonomic part which can be essentially based on any local approach. According to eq. (5), we will work with artificial potentials defined in the cartesian space \mathbb{R}^2 . More specifically, we follow [11] and superpose one *attractive* field with paraboloidic profile

$$U_a(X_p) = \frac{k_a}{2} \|X_{p,g} - X_p\|^2, \quad (7)$$

with a hyperboloidic *repulsive* field for each obstacle

$$U_r(X_p) = \begin{cases} \frac{k_r}{\gamma} \left(\frac{1}{\eta(X_p)} - \frac{1}{\eta_0} \right)^\gamma, & \text{if } \eta(X_p) \leq \eta_0 \\ 0, & \text{else,} \end{cases} \quad (8)$$

where $\eta(X_p)$ is the minimum distance of X_p from the obstacle, η_0 is the influence range of the repulsive field, and $\gamma \geq 2$ shapes the radial profile of the potential. Note that the gradient of $U = U_a + U_r$ is continuous.

It is easy to see that, in the case of m circular obstacles, the *total field* has always at least m saddle points but no isolated local minima other than the goal [13]. In the presence of obstacles of arbitrary shape, and in particular with boundary segments of zero curvature, local minima will appear with possibly large basins of attraction.

As a less conventional approach, we will also use the *vortex field* method [15]. The basic idea is to replace the antigradient of the given repulsive field with a flow rotating around the obstacle. Analytically, this amounts to moving along the direction defined by

$$F_v(X_p) = \pm \begin{bmatrix} \frac{\partial U_r(X_p)}{\partial y} \\ -\frac{\partial U_r(X_p)}{\partial x} \end{bmatrix}, \quad (9)$$

with the + sign corresponding to counterclockwise (CCW) rotation of the vortex (see Fig. 1). Note that the norm of the vortex field F_v is the same of ∇U_r , and it goes to zero at distance η_0 with continuity. The attractive field is left unchanged.

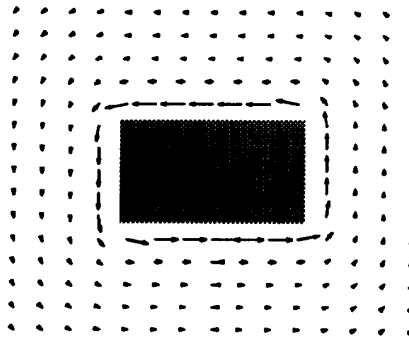


Fig. 1 – Vortex field for a rectangular obstacle

In the case of convex obstacles with domains of influence that do not overlap, it is possible to guarantee the *completeness* of the vortex field method. The choice of CW or CCW rotation for an obstacle should be made so that the relative angle α between the attractive direction $-\nabla U_a$ and F_v when entering its influence range is $\leq 90^\circ$. The method has to be complemented with a suitable *relaxation* procedure which discards the vortex—and thus the influence of the ‘bypassed’ obstacle—when the angle α goes to zero [15]. Other higher-level strategies can be devised to generalize the method to non-convex obstacles or uncertain environments [21]. We stress that the heuristics for vortex rotation and relaxation are locally defined and can be implemented

on line in a sensor-based planner. Finally, note that the vortex field method does not enforce an explicit repulsive action, so that a more conservative choice of the gains in (7-8) will be necessary to avoid the robot approaching too closely the obstacles.

4. Application to the unicycle

In this section, we apply the proposed approach to the kinematics of a unicycle (Fig. 2), where $X = (x, y, \theta)$ is the configuration vector. In this case, there is only one nonholonomic rolling constraint of the form (1):

$$\begin{bmatrix} \sin \theta & -\cos \theta & 0 \end{bmatrix} \begin{bmatrix} \dot{x} \\ \dot{y} \\ \dot{\theta} \end{bmatrix} = 0. \quad (10)$$

The kinematic model is determined as

$$\begin{aligned} \dot{x} &= \cos \theta u_1 \\ \dot{y} &= \sin \theta u_1 \\ \dot{\theta} &= u_2, \end{aligned} \quad (11)$$

where u_1 is the *driving* velocity and u_2 is the *steering* velocity. This model applies to a large class of mobile robots, including the Nomad 200™ available in our Laboratory. Nomad has a circular base of radius $R \approx 28$ cm with three wheels that translate together, controlled by one motor, and rotate together, controlled by a second motor.

According to eq. (3), the control input is chosen as

$$u = G^\#(X)\dot{X}_d = \begin{bmatrix} \cos \theta & \sin \theta & 0 \\ 0 & 0 & 1 \end{bmatrix} \begin{bmatrix} \dot{x}_d \\ \dot{y}_d \\ \dot{\theta}_d \end{bmatrix}. \quad (12)$$

This expression has a direct geometric interpretation. The driving velocity u_1 is the *orthogonal projection* of the (possibly infeasible) desired cartesian velocity along the robot main axis, while the steering velocity u_2 exactly realizes the desired rotation. Note that in the present case $G^\# = G^T$; also, unitary translational and rotational velocities are given the same weight.

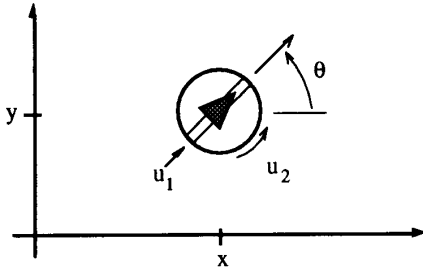


Fig. 2 – Kinematic structure of a unicycle

The desired velocity \dot{X}_d in eq. (12) comes from an incremental holonomic planner. In the following, we assume that the orientation of the mobile robot has no relevance for obstacle collision, as in the case of Nomad. As a consequence, the obstacles can be grown by R and holonomic planning will be made only for the central point of the robot†. The positional part $\dot{X}_{p,d} = (\dot{x}_d, \dot{y}_d)$ is then obtained from eq. (5) as

$$\dot{X}_{p,d} = -\nabla_{X_p}(U_a(X_p) + U_r(X_p)) \quad (13)$$

if *artificial potentials* are used, or as

$$\dot{X}_{p,d} = -\nabla_{X_p}U_a(X_p) + F_v(X_p) \quad (14)$$

for the *vortex field* method.

To complete the planning method we assign the rotational part of $\dot{X}_{\theta,d} = \dot{\theta}_d$ by specifying the form of Φ in eq. (6). For the unicycle it is convenient to use

$$\dot{\theta}_d = \text{atan2}\{\dot{x}_d, \dot{y}_d\} - \theta. \quad (15)$$

The rationale for this choice is simple. Since the unicycle can instantaneously execute linear motions only along its main axis, we force the vehicle to *align* itself with the field flow. Although the robot has circular symmetry, it is implicit in eq. (15) that the *forward* direction (i.e. the one characterized by θ) will be aligned. By defining $\text{atan2}\{0, 0\} = \theta$, the above function remains continuous along any approaching direction to the goal. The resulting command will be

$$\begin{aligned} u_1 &= k_p(\dot{x}_d \cos \theta + \dot{y}_d \sin \theta) \\ u_2 &= k_\theta(\text{atan2}\{\dot{x}_d, \dot{y}_d\} - \theta), \end{aligned} \quad (16)$$

where \dot{x}_d and \dot{y}_d are given by eq. (14). Gains k_p and k_θ are introduced to allow for additional freedom in weighting the two input commands. This is equivalent to use a weighted pseudoinverse in eq. (12).

We prove next, using a Lyapunov argument, that the motion of the unicycle under the control law (16) converges to the desired position goal $X_{p,g}$ in the absence of obstacles. Let

$$V = \frac{1}{2}\|X_{p,g} - X_p\|^2 \triangleq \frac{1}{2}\|E_p\|^2 \geq 0. \quad (17)$$

Since $\dot{X}_{p,d} = -k_a E_p$ from eq. (13) (or (14)), the time derivative of V along the closed-loop trajectories is

$$\begin{aligned} \dot{V} &= -\dot{X}_p^T E_p = -u_1 (\cos \theta \quad \sin \theta) E_p \\ &= -k_p k_a E_p^T \begin{pmatrix} \cos \theta \\ \sin \theta \end{pmatrix} (\cos \theta \quad \sin \theta) E_p \leq 0. \end{aligned} \quad (18)$$

† We are using a single control point. In the case of non-circular robots, it will be necessary to specify multiple control points on the robot body for successful motion planning.

We have that $\dot{V} = 0$ iff the row vector $(\cos \theta \quad \sin \theta)$ is orthogonal to E_p . Whenever $\dot{V} = 0$ and $E_p \neq 0$, the system dynamics becomes $\dot{x} = \dot{y} = 0$, $\dot{\theta} = \pm\pi/2$. Hence, the largest invariant set such that $\dot{V} = 0$ is $X_p = X_{p,g}$. By LaSalle's theorem, the result follows.

The above argument shows that the control law does not introduce further local minima in the configuration space of the nonholonomic robot, beside those possibly due to the holonomic field in \mathbb{R}^2 . Note that it is not possible to prove convergence for position *and* orientation, in view of the continuous differentiability of the chosen control law in the absence of obstacles.

5. Simulation Results

We simulated the proposed planner for a unicycle in a scene with circular obstacles, although both the artificial potential and the vortex field methods apply to obstacles of arbitrary shape. Input *saturation*s were included, with bounds on u_1 and u_2 respectively at 2 m/sec and $360^\circ/\text{sec}$, the bounds of Nomad scaled by a factor of 5 to speed up simulations. The steering saturation limits the reorientation capability of the vehicle. Controller gains were always set to $k_p=1$, $k_\theta=5$, while the holonomic planner parameters were $k_a=1$, $k_r=2$, $\gamma=2$, $\eta_0=2$ m. Integration was performed using the fifth order Runge-Kutta method of SIMULINK, with sampling interval $T_c=0.001 \div 0.01$ sec.

In Figs. 3 and 4, we first show for comparison two successful outputs of the *holonomic* planners obtained respectively with artificial potentials and with vortex fields. The two paths are topologically different, due to the choice of a CW vortex direction for the first encountered obstacle. The *nonholonomic* motions obtained for $\theta(0) = 0$ are shown respectively in Figs. 5 and 6, with the associated control inputs. In both cases the nonholonomic motion closely approximates the holonomic one, and the position error exponentially goes to zero in the terminal phase. Note that the unicycle in Fig. 6 undergoes initially a large reorientation, because its heading opposes the chosen vortex direction (CW) of the first obstacle. Correspondingly, the steering input saturates. This suggests more in general to keep into account the actual vehicle orientation when deciding the vortex direction for a sensed obstacle.

While navigating among obstacles, the driving velocity obtained using vortex fields is saturated at all instants. This is due to the *non-repulsive* nature of the vortex: when approaching an obstacle the robot does not experience an opposing field. On the other hand, artificial potential fields tend to slow down motion when facing an obstacle. A nonholonomic planner based on vortex fields is thus expected to generate *faster* point-to-point motions.

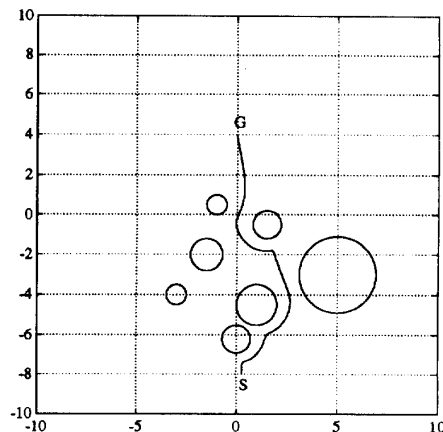


Fig. 3 – Holonomic motion using potential fields (I)

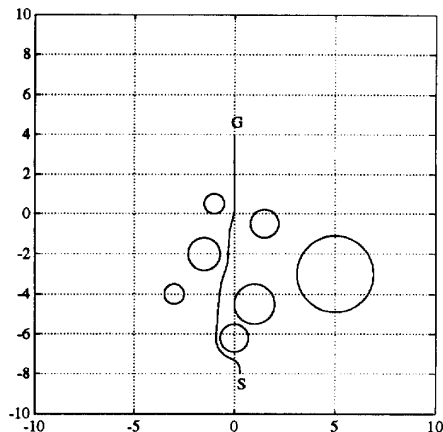


Fig. 4 – Holonomic motion using vortex fields (I)

In some cases, the performance of the two holonomic planners is drastically different. Using artificial potentials, a blocking saddle point can be met; this motivates the unsuccessful output of the nonholonomic planner in Fig. 7. Three large reorientations occur near saddle points located in front of obstacles, before the motion definitely stops. Instead, in Fig. 8 a solution path is obtained with the scheme based on vortex fields.

We have applied the proposed method to several other situations, and the performance was always satisfactory. Accurate tuning of the controller gains was not necessary, but we argue that it may be needed to handle complex situations (e.g., when only sudden reorientation would avoid collision).

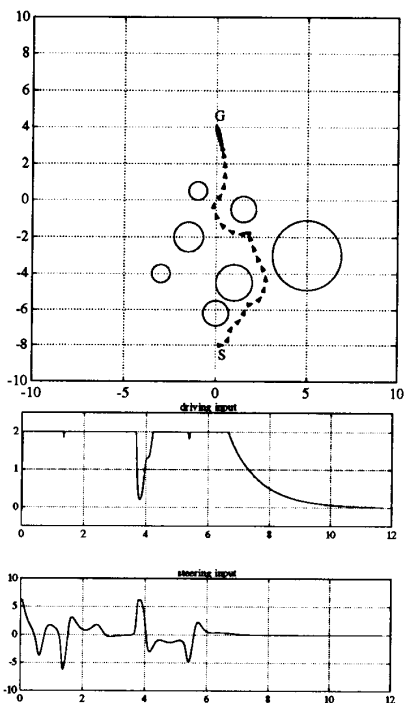


Fig. 5 – Nonholonomic planning with potential fields (I)

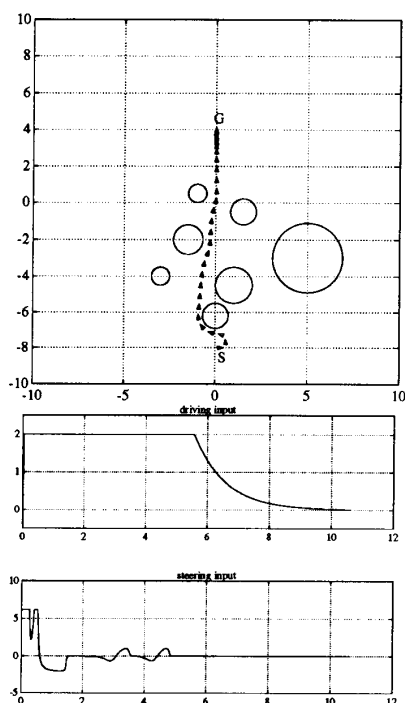


Fig. 6 – Nonholonomic planning with vortex fields (I)

6. Conclusions

We have proposed a general approach for planning the motion of wheeled mobile robots among obstacles. The nonholonomic planner consists of two basic components: a local holonomic planner generating an incremental output, and an on-line projection scheme which modifies it so to yield a feasible path together with the corresponding control inputs. As a result, a feedback scheme is obtained which can be used in real-time by feeding sensor data simply to the holonomic planner.

This approach has been applied to the case of a unicycle with circular symmetry. The artificial potential field and the vortex field methods have been elicited as holonomic planners. Their actions on desired orientation and the projection scheme have been devised so to avoid generation of additional blocking points. Simulation results show that the proposed planner performs satisfactorily in most situations.

Current work includes the derivation of explicit safety margins for the nonholonomic planner and the application to car-like mobile robots ($X = (x, y, \theta, \delta)$).

Acknowledgments

This work is supported by ESPRIT III Basic Research Project #6546 (PROMotion) and MURST 40% funds.

References

- [1] J.I. Neimark and N.A. Fufaev, *Dynamics of Nonholonomic Systems*, Transl. of Math. Monographs, vol. 33, American Mathematical Society, Providence, 1972.
- [2] J.P. Laumond, "Nonholonomic motion planning versus controllability via the multibody car system example," Rep. STAN-CS-90-1345, Stanford University, CA, 1990.
- [3] R.M. Murray and S.S. Sastry, "Nonholonomic motion planning: steering using sinusoids," *IEEE Trans. Automat. Contr.*, vol. 38, pp. 700–716, 1993.
- [4] G. Laferriere and H.J. Sussmann, "Motion planning for controllable systems without drift: A preliminary report," Rep. SYSCON-90-04, Rutgers Univ., NJ, 1990.
- [5] S. Monaco and D. Normand-Cyrot, "An introduction to motion planning under multirate digital control," *31th IEEE Conf. Decision Contr.*, Tucson, AZ, pp. 1780–1785, 1992.
- [6] R.W. Brockett, "Asymptotic stability and feedback stabilization," in *Differential Geometric Control Theory*, R.W. Brockett, R.S. Millmann, and H.J. Sussmann (Eds.), Birkhäuser, Boston, pp. 181–191, 1983.
- [7] C. Canudas de Wit and O.J. Sørđalen, "Exponential stabilization of mobile robots with nonholonomic constraints," *IEEE Trans. Automat. Contr.*, vol. 37, pp. 1791–1797, 1992.

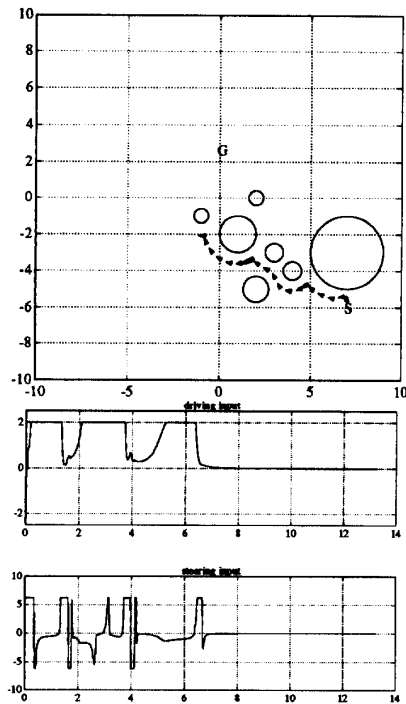


Fig. 7 – Nonholonomic planning with potential fields (II)

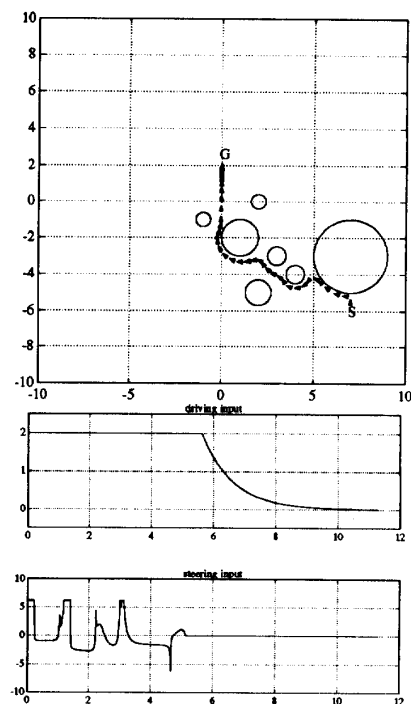


Fig. 8 – Nonholonomic planning with vortex fields (II)

- [8] C. Samson, "Time-varying feedback stabilization of car-like wheeled mobile robots," *Int. J. Robotics Res.*, vol. 12, pp. 55–64, 1993.
- [9] J.-B. Pomet, B. Thuilot, G. Bastin, and G. Campion, "A hybrid strategy for the feedback stabilization of nonholonomic mobile robots," *1992 IEEE Int. Conf. Robotics Automat.*, Nice, F, pp. 129–134, 1992.
- [10] J.C. Latombe, *Robot Motion Planning*, Kluwer Academic, Boston, 1991.
- [11] O. Khatib, "Real-time obstacle avoidance for manipulators and mobile robots," *Int. J. Robotics Res.*, vol. 5, no. 1, pp. 90–99, 1986.
- [12] R. Volpe and P. Khosla, "Artificial potential with elliptical isopotential contours for obstacle avoidance," *28th IEEE Conf. Decision Contr.*, Los Angeles, CA, pp. 180–185, 1987.
- [13] D.E. Koditschek, "Exact robot navigation by means of potential functions: Some topological considerations," *Int. Conf. Robotics Automat.*, Raleigh, NC, pp. 1–6, 1987.
- [14] J. Barraquand, B. Langlois, and J.C. Latombe, "Numerical potential fields techniques for robot path planning," *IEEE Trans. Syst., Man, Cybern.*, vol. 22, pp. 224–241, 1992.
- [15] C. De Medio and G. Oriolo, "Robot obstacle avoidance using vortex fields," in *Advances in Robot Kinematics*, S. Stifter and J. Lenarčič (Eds.), Springer-Verlag, Wien, pp. 227–235, 1991.
- [16] P. Jacobs, J.P. Laumond, and M. Taïx, "Efficient motion planners for nonholonomic mobile robots," *1991 IEEE/RSJ Int. Work. Intell. Robots Syst.*, Osaka, J, pp. 1229–1235, 1991.
- [17] J.C. Latombe, "A fast path planner for a car-like indoor mobile robot," *9th Nat. Conf. Artif. Intell.*, Anaheim, CA, pp. 659–665, 1991.
- [18] J. Barraquand, and J.C. Latombe, "Nonholonomic multibody mobile robots: Controllability and motion planning in the presence of obstacles," *1991 IEEE Int. Conf. Robotics Automat.*, Sacramento, CA, pp. 2328–2335, 1991.
- [19] A.M. Bloch, M. Reyhanoglu and N.H. McClamroch, "Control and stabilization of nonholonomic dynamic systems," *IEEE Trans. Automat. Contr.*, vol. 37, pp. 1746–1757, 1992.
- [20] O.J. Sørđalen, "Conversion of the kinematics of a car with N trailers into a chained form," *1993 IEEE Int. Conf. Robotics Automat.*, Atlanta, GA, vol. 1, pp. 382–387, 1993.
- [21] G. Oriolo, "The reactive vortex fields method for robot motion planning with uncertainty," *36th ANIPLA Annual Conf.*, Genoa, I, pp. 584–597, 1992.